

**TIME-DOMAIN IMAGING**

**Final Report**

**NASA/ASEE Summer Faculty Fellowship Program 1988**

**Johnson Space Center**

**Prepared By:** C. L. Tolliver, Ph.D., P.E.

**Academic Rank:** Professor

**University & Department:** Prairie View A&M University  
Department of Electrical Engineering  
Prairie View, Texas 77447

**NASA/JSC**

**Directorate:** Engineering

**Division:** Tracking and Communications

**Branch:** Systems Analysis Office

**JSC Colleague:** Kumar Krishen, Ph.D

**Date:** August 19, 1988

**Contract Number:** NGT 44-005-803

## Table of Contents

Abstract.....	25-3
Introduction.....	25-4
Theory.....	25-5
Experimental.....	25-11
Applications.....	25-12
Conclusions.....	25-13
Acknowledgement.....	25-14
Bibliography.....	25-15

## Abstract

The quest for the highest resolution microwave imaging and principle of time-domain imaging has been the primary motivation for recent developments in time-domain techniques. With the present technology fast time varying signals can now be measured and recorded both in magnitude and in-phase. It has also enhanced our ability to extract relevant details concerning the scattering object. In the past, the interface of object geometry or shape for scattered signals has received substantial attention in radar technology. Various scattering theories were proposed to develop analytical solutions to this problem. Furthermore, the random inversion, frequency swept holography, and the synthetic radar imaging, have two things in common: (a) the physical optic far- field approximation and (b) the utilization of channels as an extra physical dimension, were also advanced. Despite the inherent vectorial nature of electromagnetic waves these scalar treatments have brought forth some promising results in practice with notable examples in subsurface and structure sounding. The development of time-domain techniques are studied through the theoretical aspects as well as experimental verification. The use of time-domain imaging for space robotic vision applications has been suggested.

## 1. Introduction

The time-domain imaging is the synthesis of the scattered electromagnetic field distribution over an object plane. Over the past few years, an interest has developed in the use of time-domain methods or data in order to solve scattering problems. This approach has many attractive features, among them the large amount of information contained in a single pulse response and simple physical interpretations; and improvement in time-domain technology increases the interest in such an approach. The purpose of this paper is to present a short review of some techniques that have been used in the analysis of time-domain scattering. The problem of interest is the reconstruction of the shape of a convex scatter from knowledge of high frequency far field scattered from the object in response to a known incident field.

The quest for the highest resolution microwave imaging and the principle of time-domain imaging have been the primary motivation for recent developments in time-domain techniques. In the last decade, modern techniques in sampling devices and the advent of fast pulse generators have brought new technology to the practicing radar engineers in the measurements of picoseconds at a greatly reduced cost. With the present new technology, fast time varying signals can now be measured and recorded both in magnitude and in-phase.

The goals of NASA are to study the reflection coefficient at and below the surface of the tiles on the Space Shuttle with special emphasis on time-domain robotic vision applications and to continue research into problems related to the exploration of space and its applications of new technology and techniques. To obtain these goals, the Space Station shall be designed as a multi-purpose facility in which missions of long duration can be conducted and supported. These missions will include science and applications, observation, technology development and demonstration, commercial laboratories and production facilities, operational activities such as servicing/maintenance, repair of satellites, support of unmanned platforms, assembly of large space systems, and as a transportation node for transfer to other orbits and planetary missions. Automation and Robotic (A&R) is rapidly growing and it is an important technical area foreseen to increase productivity and enhance astronaut safety. The use of A&R for the Space Station can be viewed in two major areas: (1) teleoperated/robotic systems for servicing maintenance, repairs, and assembly, and (2) computerized systems to reduce the manpower requirements of planning, monitoring, diagnosis, control, and fault recovery of systems/subsystems.

In addition to increased productivity through autonomy, the A&R will result in increased operational capability and flexibility. Robotic operations for the Space Station will involve maintenance/repair of the entire structure including various subsystems, orbiter/satellite servicing, astronaut assistance, equipment transfer, docking and berthing, inspection, remote monitoring, rocket staging, telescience, and assembly of the station and large structures. To aid the astronaut in various tasks and replace him/her for some activities, robots must perform beyond the current state-of-the-art by responding to a high degree of environmental uncertainty and operational flexibility. In order to accommodate various performance goals in robots, design concepts have been proposed by Dr. Kumar Krishen of NASA and other researchers.

Today's technology enables us to extract pertinent details concerning the scattering object which conventional radar ranging lacks. The inference of object geometry or shape from scattered signals has received substantial attention in radar

technology largely due to its academic significant and the understandable commercial and military values. In the past decade, various scattering theories were proposed to develop analytical solutions to this problem. It is well known that random inversion, frequency swept holography, and the synthetic radar imaging have two things in common: (a) physical optic far-field approximation, and (b) utilization of the channels as an extra physical dimension.

Despite the inherent vectorial nature of electromagnetic waves, these scalar treatments have brought forth some promising results in practice with notable examples in subsurface and structure sounding. Recently, Dr. Kumar Krishen, of NASA/JSC, has proposed the use of time-domain imaging for space robotic vision applications. A multi-sensor approach to vision has been shown to have several advantages over the video approach.

## II. Theory

The theoretical approach outlines the basic principles of time-domain imaging relative to the synthesis of the scattered electromagnetic field distribution over an object plane. It was stressed that it is the scattered field, not the total field that is of interest, it is known by virtue of the boundary conditions, the tangential electrical field must be zero at a perfect conducting surface, where as that of the magnetic field is discontinuous by the surface current. The literature review reveals that the theory will not change and it is applicable to any arbitrary source waveform.

The scattering problems from rough surfaces is inherently different in nature from that of scattering by other bodies. Usually in the rough surface problem, an exact knowledge of the shape of the surface is neither available, nor is it of interest to the radar operator. Instead, only average properties of the surface shape enter into the problem. It is clearly understood that the last requirement rules out a boundary-value problem, since the exact boundary is not known. We are interested in the relationship between the average scattered field or radar cross section and the average surface properties. The radar cross section normalized by the area  $A$ , defined as,

$$\gamma(\theta_i) = \gamma(\theta, \theta_s, \phi) \quad (1)$$

$\theta_i$ ,  $\theta_s$ , and  $\phi_s$  are shown for the bistatic case in figure 1 below. The rough surface is assumed to consist of height variations about a mean plane, which is taken as the xy-plane. The incident wave line in the sz-plane at a polar angle.

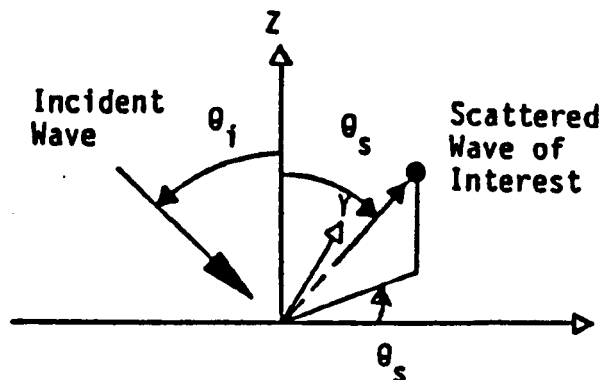


Figure 1 - THE "BISTATIC SCATTERING GEOMETRY"

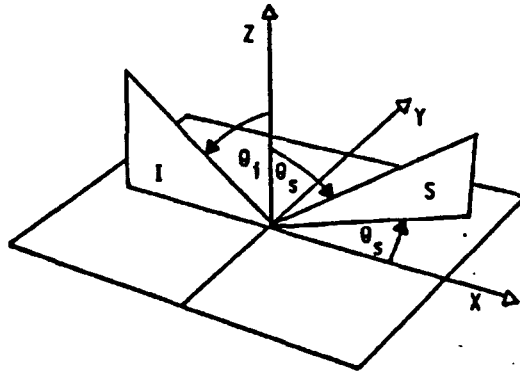


Figure 2- THE "SCATTERING GEOMETRY"

Figure 1 shows the bistatic scattering for a planar rough surface whose mean height coincides with the xy-plane and figure 2 shows the scattering geometry. I is the plane of incidence and S is the scattering plane.

The symbol  $\langle \rangle$  refers to an average and the normalized average backscattering cross section are defined as

$$\gamma(\theta_i) = \gamma(\theta, \theta, \phi) \quad (2)$$

Usually one has a specific purpose or reason for investigating scattering from a rough surface, these goals may be divided into three categories: (1) The problem of direct scattering; one wishes to know the average properties of the scattered signal or cross section when the surface properties of rough surface are known, and the scattering information is expressed in terms of the surface properties. (2) The problem of inverse scattering; one wishes to obtain statistical information about the rough surfaces from a knowledge of the average properties of the scattered field. This problem is more difficult in that there appear to be many classes of rough surfaces producing the same average scattering cross section as a function of the bistatic scattering angle and wavelength.

The radar cross section (scattered field) can be expressed as  $4\pi$  times the power delivered per unit solid angle in the direction of the receiver divided by the power per unit area incident at the target. The factor  $4\pi$  enters from the definition of a solid angle. Assuming for the moment that the propagation path between the target and the receiving system is lossless, then this power ratio may be expressed as

$$4\pi r^2 \frac{(E^s \cdot E^{s*})}{(E^i \cdot E^{i*})} = 4\pi r^2 \frac{(H^s \cdot H^{s*})}{(H^i \cdot H^{i*})} \quad (3)$$

Where  $E^s$  and  $H^s$  are the scattered electric and magnetic fields, respectively and  $E^i$  and  $H^i$  are the incident fields. The scattered field is defined to be the difference between the total field (with the target present) and the incident field. This is summarized as

$$E^s = E^T - E^i \quad (4)$$

Finding the cross section ( $\sigma$ ) now becomes a problem in electromagnetic field theory. In order that the cross section be independent of  $r$ , it is desirable to let  $r$  in Eq. 3 become arbitrarily large (scalar definition, not a tensor function).

$$\sigma = 4\pi \lim_{r \rightarrow \infty} r^2 \frac{(E^s \cdot E^{ts})}{(E^i \cdot E^{is})} = 4\pi \lim_{r \rightarrow \infty} r^2 \frac{(H^s \cdot H^{ts})}{(H^i \cdot H^{is})}. \quad (5)$$

To compute the scattered field, one sometimes computes the current induced on the target and then treats the target current distribution in terms of an equivalent aperture distribution. Antennae are often compared to an isotropic antenna, that is, an antenna which radiates uniformly in all directions.

In the problem of clutter, returns from terrain are not wanted. However, in many cases the presence of clutter is unavoidable along with the desired signal. One can detect and analyze the desired signal significantly better if more is known about the properties of the clutter or noise produced by terrain scattering. It is noted that surface information is generally known, and the properties of the scattered signal are related to Eq. 3.

The Fourier transform was used in this analysis and it was shown that space-time equations can be readily derived from their space-frequency counterparts. The equations derived will be applicable to field of arbitrary time variation.

The source signal is related to the fourier transform,  $F(w)$ , by:

$$(a) \quad F(w) = \int_{-\infty}^{\infty} f(t) e^{j\omega t} dt \quad (b) \quad f(t) = \frac{1}{2\pi} \int_{-\infty}^{\infty} F(w) e^{-j\omega t} d\omega. \quad (6)$$

The upper case lettering are used for the transformed functions unless otherwise noted. The wave number  $k = w/c$ , where  $c$  is the speed of light in the medium.  $\alpha$  and  $\beta$  are the direction cosines of the vector  $r$  projected onto the  $xy$ -plane with  $\alpha = \sin\theta \cos\phi$ ,  $\beta = \sin\theta \sin\phi$ .

It can be assumed that the field distribution over the antenna apertures and object plane is space-time separable; the field strength of each radiating element observed at some point  $r$  is  $e(r,t) = e(r) f(t - r/c)$ , the field strength, and  $f(t - r/c)$  is the sine wave traveling at the speed of light.

Assume the scatter in figure 2 to be placed in a far field, such that the assumption of uniform impinging planewave over the object can be obtained by the application of the far field Kirchhoff-Huygens principle.

The basic principle of time-domain imaging over an object plane has been formulated and discussed by many researchers. It was not until 1983 when Wolfgang-M Boerner developed a finite difference-time domain method (FD-TD) with a near field to far field transformation using field equivalence, that a method to treat realistic scattering problems effectively was developed. In this method, the scattering problem is analyzed in two steps by treating the relatively complex near field region and the relatively simple far field region separately. The method involves first the determination of equivalence electric and/or magnetic current tangential to a virtual surface surrounding the scatter of interest by using the FD-TD method for a given external illumination. The computed near-field equivalent currents are then transformed to derive the far-field scattering problem and the radar cross section. Since the FD-TD method can deal with dielectric, permeable, and in homogeneous

materials in a natural manner, it is possible to incorporate most of the physics of wave interaction with any complex scatter of interest

The Kirchhoff-Huygens principle deals with scattering, but the process is not as sensitive in analyzing scattering as the method put forth by Wolfgang-M Boerner, et al. The Kirchhoff-Huygens method deals with far field scattering, whereas Wolfgang-M Boerner treats both far field and near field scattering.

The theory involving finite difference-time domain (FD-TD) is not without limitation. This method is based upon the physical optics approximation which is valid for scatter whose dimension is significantly larger than the incident wave length and is independent of polarization.

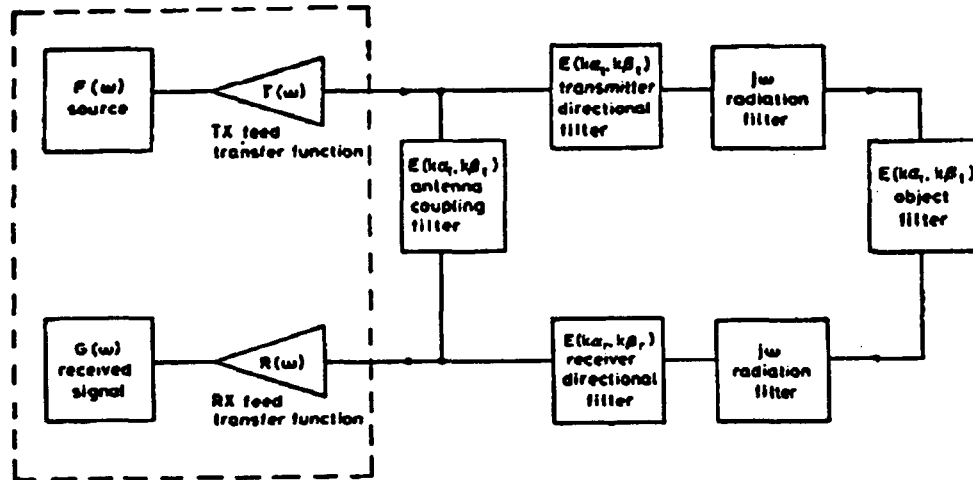


Figure 3 - SCHEMATIC DIAGRAM OF THE TARGET IMAGING SYSTEM

$$I(w) = \frac{\cos \theta}{4\pi cr_o} jw F(w) T(w) \int_{-\infty}^{\infty} \int_{-\infty}^{\infty} e(x, y) \exp[-jk(\gamma_o - \alpha_1 x - \beta_1 y)] dx dy. \quad (7)$$

$$I(w) = \frac{\cos \theta}{4\pi cr_o} jw F(w) T(w) E_t(k\alpha_1, k\beta_1) \exp[-jkr_o]. \quad (8)$$

Where  $E_t(k\alpha_1, k\beta_1)$  is the transmitting-antenna anisotropic directional filter and  $r$  is the distance between the transmitter aperture and an object plane taken as reference.

The second application of the Kirchhoff-Huygens principle and fixed phase evaluation can be shown with little calculus that the received waveform,  $g(t)$ , is

$$g(t) = \text{const} \int_{-\infty}^{\infty} F(w) T(w) R(w) [E_o(k\alpha_o, k\beta_o) + (jw)^2 E_t(k\alpha_1, k\beta_1) E_r(k\alpha_r, k\beta_r) E_o(k\alpha_o, k\beta_o) e^{-jkr}] e^{-jw t} dw. \quad (9)$$

where the direction cosine, the constant and the distance are dependent on the imaging geometry.

For the monostatic case commonly encountered (see figure 4 below), the transmitter and receiver coincide. In particular, if the phase center of the object is on boresight which suggests that the target is closely tracked, Eqn. 9 can be considerably simplified to yield:

$$g(t) = \text{const} \int_{-\infty}^{\infty} F(w) T(w) R(w) [E_o(k\alpha_o, k\beta_o) + (jw)^2 E_t(0, 0) E_r(0, 0) E_o(k\alpha_o, k\beta_o) e^{-2jkr}] e^{jw t} dw. \quad (10)$$



The delineation of the objective response is exercised as follows: First, the time response in the absence of any scattering objects is recorded.

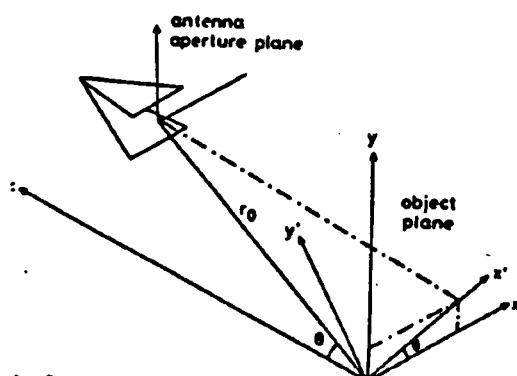


Figure 4 - IMAGING GEOMETRY

$$(a) \quad x = \frac{\alpha x' + \beta y'}{\sqrt{\alpha^2 + \beta^2}}$$

$$(b) \quad y = \frac{\beta x' - \alpha y'}{\sqrt{\alpha^2 + \beta^2}}$$

$$(c) \quad \cos \theta = \frac{\alpha}{\sqrt{\alpha^2 + \beta^2}}$$

$$(d) \quad \sin \theta = \frac{\beta}{\sqrt{\beta^2 + \alpha^2}}$$

#### IMAGING GEOMETRY EQUATIONS

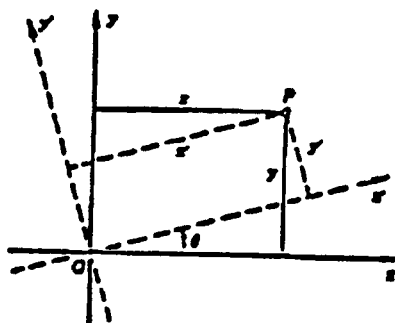


Figure 5a

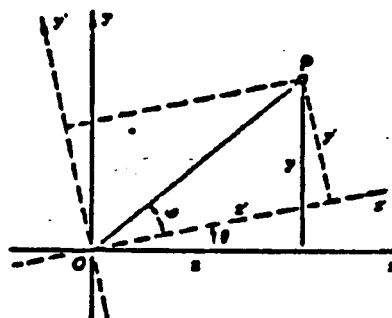


Figure 5b

$$(f) \quad \begin{aligned} x &= x' \cos \theta - y' \sin \theta, \\ y &= x' \sin \theta + y' \cos \theta, \end{aligned}$$

$$(g) \quad \begin{aligned} x' &= x \cos \theta + y \sin \theta, \\ y' &= -x \sin \theta + y \cos \theta. \end{aligned}$$

$$(h) \quad \frac{x}{|OP|} = \cos(\phi + \theta), \quad x = |OP| \cos(\phi + \theta) = |OP|(\cos \phi \cos \theta - \sin \phi \sin \theta).$$

$$(i) \quad \sin \phi = \frac{y'}{|OP|} \quad \text{and} \quad \cos \phi = \frac{x'}{|OP|}$$

#### THE ROTATION TRANSFORMATION

The antenna's coupling filter is removed when the signal is subtracted from other records with the scatter present. Multiple path scattering between the object and surrounding obstacles can be gaited out in time when sufficiently large space is given. By definition,

$$E_o(k\alpha_o, k\beta_o) = \int_{-\infty}^{\infty} \int_{-\infty}^{\infty} e_o(x, y) \exp[2jk(\alpha_o x + \beta_o y)] dx dy. \quad (11)$$

The system kernel,  $K(w)$ , can be obtained once the coupling term has been eliminated.

$$K(w) = \cos^2(jw)^2 F(w) T(w) R(w) E_t(0, 0) E_r(0, 0) E_o(0, 0) e^{-2jkr_o}. \quad (12)$$

The use of mathematical techniques, provides an opportunity for the backscattering waveform to be simplified. To give the system kernel,  $K(w)$ , and to obtain the electrical field strength in frequency domain and by the projection theorem, the response obtained is equivalent to a slice in the two dimension fourier plane (figure 4), which is a representation

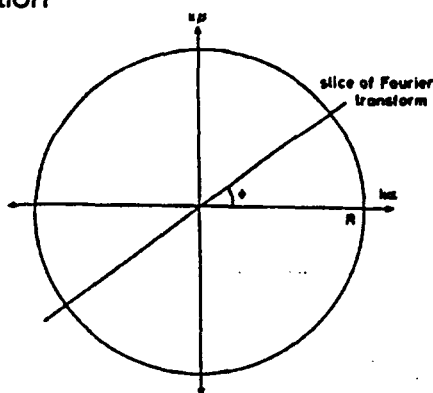


Figure 4 - ONE-DIMENSIONAL TARGET FREQUENCY RESPONSE

of the one-dimensional target frequency response in the two- dimensional fourier plane at a particular viewing direction. Equation 9 becomes

$$E(k\alpha, k\beta) = \frac{G(w)e^{2jkr_o}}{k(w)} \quad (13)$$

The application of the inverse fourier transform of equation 13 yields the object impulse response

$$\int_{-\infty}^{\infty} E(k, o) e^{-jw(t - 2x' \sin \frac{\theta}{c})} dw = e(t - 2x' \sin \frac{\theta}{c}) \quad (14)$$

which can be considered as a series of scans across the object surface where each is an integral of the object field which is orthogonal to the viewing direction. The spatial resolution is thus achieved by the utilization of the time channel and the minimal resolvable dimension  $\Delta x$  is related to the sampling interval  $T$ , namely

$$\Delta x = \frac{cT}{2\sin(\theta)} \quad (15)$$

a different impulse response is obtained by the rotation of the object plane about the z-axis, which corresponds to another slice in the Fourier plane. Further rotation over a 180 degrees span will fill up the entire Fourier plane.

The two-dimension object field distribution is recovered, namely the reconstruction strength,  $e(x, y)$

$$e(x, y) = \frac{1}{4\pi^2} \int_0^\pi d\phi \int_{-R}^R \frac{R}{\pi} E(k\alpha, k\beta) \sin\left(\frac{k}{R}\pi\right) e^{-2jk(\alpha x + \beta y)} dk \quad (16)$$

a smoothing filter  $A(k\alpha, k\beta)$  is introduced to compensate for the amplification of high frequency component due to the factor  $k$  in field strength equation [Eq. 16]. It is not necessary to have  $A$ , for noise free data. For practical numerical evaluation, the finite sampling rate will impose an upper limit,  $R$ , to the wave number  $k$ . To eliminate abrupt cutoff, which would cause ringing in the resultant image, it is necessary to introduce equation 16, to yield a smoothed image, equation 17

$$A(k\alpha, k\beta) = \sin\left(\frac{k\pi R}{\left(\frac{k\pi}{R}\right)}\right) \quad (17)$$

$$e(x, y) = \frac{1}{4\pi^2} \int_0^\pi d\phi \int_{-R}^R \frac{R}{\pi} E(k\alpha, k\beta) \sin\left(\frac{k}{R}\pi\right) e^{2jk(\alpha x + \beta y)} dk \quad (18)$$

and is the basis of our reconstruction field strength.

### III. Experimental

The government, private, and public sector have always had a need for time-domain imaging. This area of research did not surface until early 1962. The new and old researchers in electromagnetic field theory and other scientist provided many theoretical ideals on direct and indirect scattering. It was observed that these researchers did not have an insight into the circuit design, arrangement of apparatus and development of the necessary experiments to verify and determine the applications of the existing theory.

Back scattering from metallic objects was experimentally observed and the signal processing technique for extracting the object response was performed in 1985 by Yeung and Evans. It was not until this time when Yeung and Evans put the existing theory coupled with experimental verification together and made a projection of the long over due applications. After carefully reviewing the literature and the experimental verification provided by these two researchers, it was observed that applications of time-domain imaging is applicable to many aspects of the private and public sector, but the immediate and long range beneficiaries are NASA and the military.

Recently, Dr. Kumar Krishen of NASA/JSC has proposed the use of time-domain imaging for space robotic vision application. It has been shown that space objects are covered with heat shields, (dielectric materials), and microwave penetrate through these shields. A multi-sensor approach to this robotic vision application has been shown to have several advantages over a video approach.

The authors of this paper will use the necessary apparatus and experimental arrangement of Yeung and Evans to demonstrate the viability of impulse imaging. Verifying the experimental results should give us confidence in the validity of the theoretical method over a broad range of angles and the enormous experimental

potential of time-domain techniques in radar- scattering measurements. After scrutinizing the theory and experimental results of Yeung and Evans, the authors of this paper will look into time-domain robotic vision application and the effects of pulse width, polarization, look angles, and phase images of robotic vision coupled with, conducting experiments to verify the application of the existing theory and experiment.

The target size employed in these experiments are comparable to the source pulse width, and it is well known that electrical shape of objects at low frequencies could be considerably different from the physical shape.

Finite source rise-time (hence limited bandwidth) and insufficient source power are the major difficulties for achieving the highest resolution and sharp images. The system kernel involves the differentiation of the source waveform, and this adds uncertainties in the determination of low-frequency components which is usually manifested as a slowly varying baseline in the deconvolved result.

#### IV. Applications

In 1986, a summary of goals and objectives were recommended by the NASA's Advanced Technology Advisory Committee (ATAC) [1]. The robotic applications set up by the Committee are: (a) Teleoperation of mobile remote manipulator with collision avoidance. (b) Mobile multiple-arm robot with dexterous manipulators to inspect and exchange orbital replaceable units. (c) Systems designed to be serviced, maintained, and repaired by robots.

The current remote manipulator system (RMS) will be used to manipulate initial station assembly in the Space Shuttle. Further versions of the RMS will be employed to assemble Space Station and satellite.

NASA/JSC is currently developing an early robot, the extra- vehicular astronaut (EVA) retriever, to perform as an aid to an EVA/man maneuverable unit (MMU) astronaut and retrieve the astronaut if circumstances dictate such an operation.

In the development of the space vision systems cost effectiveness, speed, small size, lightweight, high reliability and flexibility, and ease of operation must be considered. Microwave techniques of time-domain imaging is one of the tools to achieve the above purposes.

Robotic technology has been widely utilized by NASA to explore space; however, one of the most challenging problems to deal with is robotic vision. Vision is needed in fixed locations to keep track of location of objects, to pick and place machines/systems, and to monitor performance of non-automatic systems. Indeed, vision provides intelligence and flexibility in locating automated and non-automated machines.

As the robotics era dawns in space, vision will provide the key sensory data needed for multi-faceted intelligent operations. In general, the 3D scene/object description along with location, orientation, and motion parameters will be needed. Sensor complements may include both active and passive microwave and optical types with multi-function capability. The fusion of the information from these sensors to provide accurate parameters for robots provides by far the greatest challenge in vision. Furthermore, the compression, storage, and transmission of the

information associated with multi-sensor capability require novel algorithms and hardware for efficient operation.

The vision requirements for space robotics are characterized by environmental factors and tasks the robot has to perform. The natural space environment consists of intense light and dark periods. At a normal Space Station altitude, the sunlight intensity will fluctuate above 60 minutes of extreme brightness and 30 minutes of darkness. Furthermore, due to the absence of atmosphere, light is not diffused/scattered. The ubiquity of white surfaces intensifies the problem of relying on photometric data for object identification/discrimination. A secondary source of concern effecting vision is the absence of gravity. For free flying and tethered objects may be found due to the lack of disturbance caused by aerodynamic and gravitational forces.

The unpredictable nature of maintenance and repair tasks creates a problem in the development of the capability/design of space robots. The vision capabilities must be adaptive/versatile to accommodate these uncertainties

The quest for the highest resolution microwave imaging and the principle of time-domain imaging has been the primary motivation for recent developments in time-domain techniques. In the last decade, modern techniques in sampling devices and advent fast pulse generators has brought new technology to the practicing radar engineers in the measurements of picoseconds at a greatly reduced cost. With the present technology, fast time varying signals can now be measured and recorded both in magnitude and in-phase.

Conventional radar ranging has been enhanced by modern technology's ability to extract details about the scattering object.

## V. Conclusions

In this paper various research approaches to time-domain imaging have been reviewed with particular emphasis on the mathematical and physical approximations made in them.

Yeung and Evan dealt with the Kirchhoff-Huygens Principles, which deal with far field scattering whereas Boerner dealt with both far field and near field scattering. We feel that the far and near field scattering technique is a better approximation, particularly when applied to a scattering object that is not a perfect conductor.

Based on the theoretical and experimental verification provided by these authors it is necessary that future research be done so as to go beyond the existing approximations of Boerner, et al. For instance, a non-trivial generalization, should apply to conductivity and non-conducting targets.

### Acknowledgement

The authors wish to thank Mr. R. S. Sawyer of NASA/Johnson Space Center for his encouragement the past two summers and continued support of the research reported in this paper.

## Bibliography

Advancing Automation and Robotics Technology for the Space Station and for the U.S. Economy, Progress Report 3. NASA Advanced Technology Advisory Committee, Washington, D.C., September, 1986.

Space Station Automation Study, Automation Requirements Derived from Space Manufacturing Concepts, Volume I and II, General Electric, November 27, 1984

Automation Study for Space Station Subsystems and Mission Ground Support-Final Report, Hughes Aircraft Company, November 1984.

Space Station Automation Study, Final Report, Volume I and Volume II, Martin Marietta, November 1984.

Space Station Automation and Robotics Study, Final Report, Boeing Aerospace Company, November 1984.

Satellite Services System Analysis Study, Executive Summary, Final Briefing, Grumman Aerospace Corporation, July 22, 1981.

NASA Space Station Automation: AI Based Technology Review, Executive Summary, SRI International, March 1985.

Bachman, C.G., *Radar Targets* (Gover Pub. Co. Ltd., 1982), pp. 110-113.

Beckman, P. and Spizzichino, A., *The Scattering of Electromagnetic Waves from Rough Surfaces*. (The Macmillan Co., 1963), pp. 10-28, 178-181.

Bennett, C.L., and Ross, G.F., *Time domain electromagnetics and its applications*, *ibid.*, 1978, 66, pp. 299-318.

Boerner, W.M., Ho, C.M., and Foo, B.Y., *Use of Radon's projection theory in electromagnetic inverse scattering*, *IEEE Trans.*, 1981, AP-29, pp. 336-341.

Chan, C.K., and Farhat, N.H., *Frequency swept tomographic imaging of three dimensional perfectly conducting objects*, *ibid.*, 1981, AP-29, pp. 312-319.

Censor, Y., *Finite series-expansion reconstruction methods*, *ibid.*, 1983, 71, pp. 409-419.

Evans, S., and Kong, F.N., *Gain and effective area of impulse antenna*, *Third International Conference on Antenna and Propagation*, ICAP 83, Norwich, England, april 1983, pp. 421-424.

Fialkovskiy, A.T., *Diffraction of planar electromagnetic waves by a slot and a strip*, *Radio Eng. Electron.*, 1966, 11, pp. 150-157.

Kennaugh, E.M. and Moffatt, D.C., *Transient and impulse approximations*, *Proc. IEEE*, 1965, 53, pp. 893-901.

Kong, F.N., Ph.D. Dissertation, Cambridge University, August 1983, Chap. 8.

Lewitt, R.M., *Reconstruction algorithms: transform methods*, *Proc. IEEE*, 1983, 71, pp. 390-408.

Reader, H.C., Evans, S., and Yeung, W.K., *Illumination of a rectangular slot radiator over a 3 Octave bandwidth*, Fourth International Conference on Antennas and Propagat., ICAP 85, 1985, pp. 223-226.

Ruck, G.T., Barrick, D.E., Stuart, W.D., and Krichbaum, C.K., *Radar Cross Section Handbook* (Plenum Press, 1970), pp. 671-689. Schubert, K. A., Young, J.D., and Moffatt, D.L., *Synthetic Radar Imaging*, *ibid*, 1977, AP-25, pp. 477-483.

Tiknonov, A.N. and Arsenic, V.Y., *Solutions of ill-posed problem* (Winton-Wiley, New York, 1977)

Yeung, W.K. and Evans, S., *Time-domain microwave target imaging*, Proc. IEEE, 1985, 132, pp. 345-350.